An ordered cubic *Im*3*m* mesoporous Cr–TiO_2 visible light photocatalyst

Jimmy C. Yu,*[a] Guisheng Li,[a] Xinchen Wang,[b] Xianluo Hu,[a] Cheuk Wan Leung[a] and Zhendong Zhang[a]

Received (in Cambridge, UK) 8th March 2006, Accepted 8th May 2006
First published as an Advance Article on the web 25th May 2006
DOI: 10.1039/b603456j

An ordered and well-crystallized cubic *Im*3*m* mesoporous Cr–TiO_2 photocatalyst with superb performance under visible light has been fabricated.

Cubic mesoporous TiO_2 possesses an interwoven and continuous uniform 3D pore system. This favors mass-transfer kinetics, and the photocatalyst has great potential for environmental applications.[1,2] However, the anatase TiO_2 semiconductor has a relatively large band gap of 3.2 eV, corresponding to a wavelength of 388 nm.[3] The requirement for UV excitation impedes the development of solar-driven photocatalytic systems. It is known that the response of TiO_2 can be extended to the visible light region by doping.[3,4] Doping can also bring other advantages, such as a high anatase crystallinity, large surface area and a low recombination rate of electrons and holes.[5] Despite the apparent benefits, there is no report to date of the synthesis of a transition metal-doped 3D mesoporous TiO_2 visible light photocatalyst. We utilized the EISA (evaporation-induced self-assembly) method to build the 3D framework.[6] The doping of Cr into TiO_2 was achieved by adding chromium(III) nitrate and titanium tetrachloride together as precursors. Compared to that of pure mesoporous TiO_2, the resulting ordered cubic *Im*3*m* mesoporous Cr–TiO_2 exhibited superior visible light photocatalytic activity.

To synthesize the cubic *Im*3*m* mesoporous Cr–TiO_2, 1.5 g of poly(alkyleneoxide) block copolymer, $HO(CH_2CH_2O)_{106}(CH_2CH(CH_3)O)_{70}(CH_2CH_2O)_{106}H$ (abbreviated as $EO_{106}PO_{70}EO_{106}$: Pluronic F-127, BASF), was dissolved in 19 mL of ethanol (EtOH) containing 0.15 g $Cr(NO_3)_3{\cdot}9H_2O$. To this solution was added 0.015 mol of titanium tetrachloride (Aldrich) with vigorous stirring for 0.5 h. The resulting sol solution was gelled in an open petri dish at 40 °C in air for 4 days, during which time the inorganic precursor hydrolysed and polymerized into a metal oxide network. The as-prepared transparent sample was then calcined at 400 °C for 5 h in air to remove the surfactant species.

Low- and wide-angle X-ray diffraction measurements were carried out using a Bruker D8 Advance X-ray diffractometer with Cu-Kα radiation. The N_2-sorption isotherms were recorded at 77 K using a Micromeritics AsAP 2010 instrument. The Brunauer–Emmett–Teller (BET) approach was used for the determination of the surface area. Standard transmission electron microscopy images and the chemical composition were recorded using a CM-120 microscope (Philips, 120 kV) coupled with an EDX spectrometer (Oxford Instruments). High-resolution transmission electron microscopy (HRTEM) was recorded by a JEOL-2010F at 200 kV. The reflectance spectra of the samples over a range of 200–700 nm were recorded by a Varian Cary 100 Scan UV-vis system (USA) equipped with a Labsphere diffuse reflectance accessory.

The photocatalytic degradation of methylene blue was carried out in an aqueous solution at ambient temperature. Briefly, in a 100 ml beaker, 0.08 g of mesoporous Cr–TiO_2 was mixed with an 80 mL aqueous solution containing 10 ppm methylene blue. The mixture was stirred for 1 h until reaching adsorption equilibrium. The catalytic degradation of methylene blue was initiated by irradiating the reaction mixture with a visible light source consisted of a 300 W tungsten–halogen spotlight and a filter that restricted the illumination to a 400–660 nm range.[7] Oxygen under atmospheric pressure was bubbled through the reaction continuously. Photodegradation was monitored by measuring the absorbance of the methylene blue at its maximum using a UV-vis system.

Fig. 1a shows the nitrogen adsorption–desorption isotherms (inset) and pore size distribution plots for the mesoporous TiO_2 and Cr–TiO_2. Both samples exhibit a type-IV isotherm, being representative of mesoporous solids. The specific surface area of the Cr–TiO_2 sample is 135 $m^2\ g^{-1}$ using the BET method. The pore diameter of the Cr–TiO_2 is 3.2 nm (estimated using the

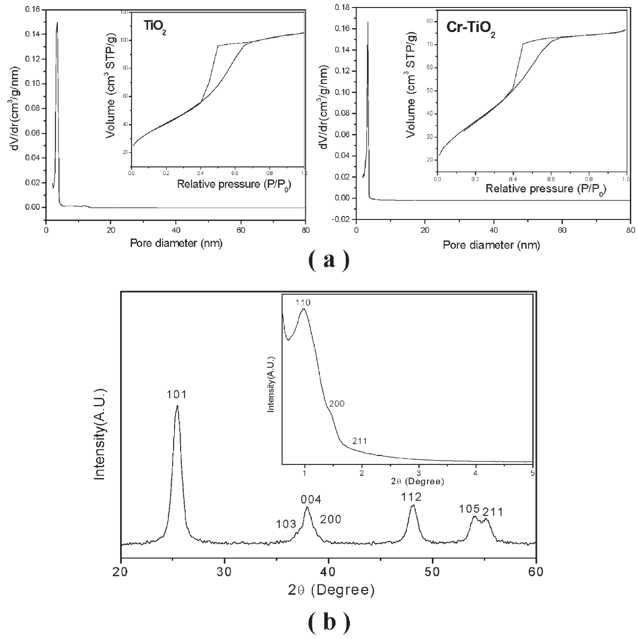

Fig. 1 (a) N_2-sorption isotherms (inset) and corresponding pore size distribution curves for pure TiO_2 and Cr–TiO_2. (b) XRD patterns for Cr–TiO_2 in wide-angle and small-angle (inset) regions.

---

[a] *Department of Chemistry and Environmental Science Programme, The Chinese University of Hong Kong, Shatin, New Territories, Hong Kong, China. E-mail: jimyu@cuhk.edu.hk; Fax: +852 2603-5057; Tel: +852 2609-6268*
[b] *Research Institute of Photocatalysis, College of Chemistry and Chemical Engineering, Fuzhou University, Fuzhou 350002, China*

desorption branch of the isotherm) with a very narrow pore size distribution. The TiO_2 samples possess a virtually identical average pore diameter (3.4 nm) and specific surface area (142 $m^2\ g^{-1}$), taking into consideration the typical uncertainty of 5% for BET surface area measurements.[8] The doping with Cr^{3+} results in a slight decrease in the pore volume of TiO_2 from 0.159 to 0.135 $cm^3\ g^{-1}$. These results illustrate that the doping with Cr^{3+} ion does not significantly change the textural properties of TiO_2. The Cr^{3+} ions are embedded in the TiO_2 network of the mesoporous pore walls, and the pore channels remain open. Such an open mesoporous architecture, with a large surface area and 3D-connected pore system, plays an important role in catalyst design for its ability to improve the molecular transport of reactants and products.[9] Wide-angle X-ray diffraction (WXRD) and small-angle X-ray diffraction (SXRD) were used to identify the crystalline phase and mesostructural ordering of the Cr–TiO_2 sample. Fig. 1b shows the WXRD pattern; the diffraction peaks at 2θ of 25.3, 36.9, 38.2, 38.6, 48.1, 53.5 and 55.6° are attributed to anatase TiO_2 (JCPDF 84–1285). Here, no crystalline phase involving chromium oxides can be observed, which further confirms that all Cr^{3+} ions are dispersed in the TiO_2 network. The radius of Cr^{3+} is 0.76 Å, which is very close to that of Ti^{4+} (0.75 Å). Substitution of Ti^{4+} by Cr^{3+} would therefore not cause much stress in the crystalline lattice. The particle size for the catalyst was found to be 11.5 nm, as estimated from the FWHM of the TiO_2 (101) peak using the Sherrer formula. This indicates that the Cr–TiO_2 sample is composed of well-crystallized anatase. Crystallization of the TiO_2 mesoporous framework is a key factor for applications of the sample in devices that utilize its semiconductor properties, such as photocatalysts.[10] From the lower 2θ region (Fig. 1b, inset), a strong peak at 0.98° (2θ) can clearly be seen in the XRD pattern, together with relatively weak peaks at 1.45 and 1.83°. These diffraction peaks are the (110), (200) and (211) reflections of the cubic *Im*3*m* mesophase. The sharp and strong (110) peak, together with the presence of the (200) and (211) peaks, further demonstrates that the Cr–TiO_2 sample is well-organized at the meso scale.

The transmission electron microscopy (TEM) images support the WXRD and SXRD results. A long-range order structure is readily observed in the Cr–TiO_2 composite (Fig. 2a). The image also shows that no trace of a chromium oxides phase can be found in the sample. Fig. 2b shows the HRTEM image of the Cr–TiO_2 nanocomposite. The nanocrystalline nature of anatase TiO_2 (ellipses) is well defined. The particle size of the TiO_2 nanocrystal is about 10 nm, which is consistent with that calculated from the XRD data. Such high anatase crystallinity in the mesoporous TiO_2 is highly desirable in photocatalysis.[11]

Meanwhile, the composition of the Cr element map is shown in Fig. 2c; the white areas representing the Cr distribution and the black areas, marked with circles, corresponding to the pores of the mesoporous Cr–TiO_2. As illustrated by the map, virtually all Cr^{3+} ions are highly dispersed in the pore walls of the mesoporous TiO_2. This map confirms that Cr^{3+} is well embodied into the TiO_2 mesoporous network through substitution of Ti^{4+} from the TiO_2. Furthermore, the EDX spectroscopy measurements (Fig. 2d) show a Cr/Ti molar ratio of about 0.025 : 1.

The UV-vis absorption spectra of the mesoporous TiO_2 and Cr–TiO_2 samples are shown in Fig. 3. The inset in Fig. 3 shows the optical absorption edge (in eV). The optical band edge of the mesoporous Cr–TiO_2 (about 2.5 eV) exhibits a marked red-shift with respect to that of pure TiO_2. This can be assigned to the charge-transfer band $Cr^{3+} \rightarrow Ti^{4+}$ or $4A_{2g} \rightarrow 4T_{1g}$ of Cr^{3+} in an octahedral environment. Meanwhile, the $4A_{2g} \rightarrow 4T_{2g}$ d–d transitions of Cr^{3+} result in a broad absorption band above 620 nm.[12] The enhanced ability to absorb visible light makes this mesoporous TiO_2 an effective photocatalyst for solar-driven applications.

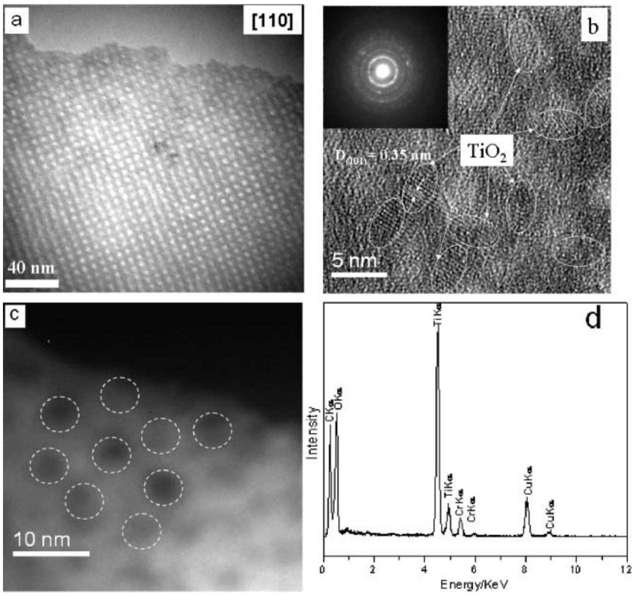

Fig. 2 (a) Standard TEM and (b) HRTEM images of Cr–TiO_2. The inset in (b) shows the diffusion rings for the anatase nanocrystallinity of (a) and (b). (c) The chemical map of Cr–TiO_2 (white areas correspond to the Cr distribution). (d) The energy dispersive X-ray (EDX) analysis results for (a). Note: Cu and C come from the supporting carbon-coated copper grid.

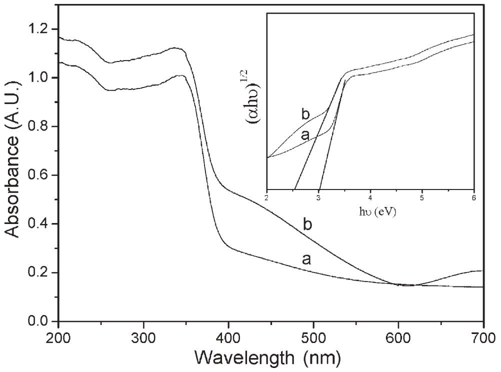

Fig. 3 UV-visible absorption spectra of (a) pure TiO_2, and (b) Cr–TiO_2.

To evaluate and compare the photocatalytic performance of the mesoporous TiO_2 samples, the decomposition of methylene blue was used as a photoreaction probe. Results of the photocatalytic evaluation are summarized in Fig. 4. The pure mesoporous TiO_2 is ineffective but the mesoporous Cr–TiO_2 shows a very high decomposition rate. This must be due to the Cr^{3+} doping, which allows activation of the mesoporous TiO_2 sample in the visible light region. The excellent photocatalytic performance is also related to the open mesoporous architecture with a large surface area, good anatase crystallinity and a 3D-connected pore system.

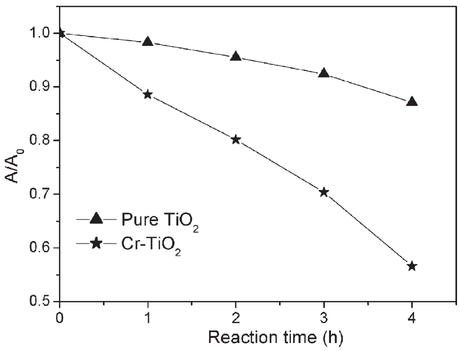

Fig. 4 A comparison of the photoactivities of pure TiO_2 and Cr–TiO_2. *A* is the absorbance of methylene blue (λ_{max} = 664 nm) and A_0 is the initial absorbance.

It is known that chemical reactions are most effective when the transport paths through which molecules move into or out of the nanostructured materials are included as an integral part of the architectural design.[9] The 3D-interconnected mesochannels in the cubic mesoporous Cr–TiO_2 composite serve as efficient transport paths for reactants and products in photocatalytic reactions.[2]

In summary, a novel highly effective visible light-sensitive photocatalyst was prepared by doping chromium ions (Cr^{3+}) into a mesoporous TiO_2 framework by using the EISA method. The resulting homogeneous mesoporous Cr–TiO_2 nanoarchitecture possesses well-crystallized anatase phases, a large specific surface area, a uniform pore size, and a 3D-accessible framework. The Cr^{3+} ions are well confined in the anatase nanocrystal framework that compose the mesopore walls. Such an interaction between Cr^{3+} ions and the TiO_2 framework is key for the enhancement of photoactivity in the visible light region.

The work described in this paper was supported by a grant from the Research Grants Council of the Hong Kong Special Administrative Region (project no. 402904).

Notes and references

1 S. Rodrigues, K. T. Ranjit, S. Uma, I. N. Martyanov and K. J. Klabunde, *Adv. Mater.*, 2005, **17**, 2467.

2 J. C. Yu, X. C. Wang and X. Z. Fu, *Chem. Mater.*, 2004, **16**, 1523.

3 M. Anpo and M. Takeuchi, *J. Catal.*, 2003, **216**, 505.

4 (*a*) J. C. Yu, W. K. Ho, J. G. Yu, H. Y. Yip, P. K. Wong and J. C. Zhao, *Environ. Sci. Technol.*, 2005, **39**, 1175; (*b*) H. X. Li, J. X. Li and Y. N. Huo, *J. Phys. Chem. B*, 2006, **110**, 1559.

5 H. X. Li, G. S. Li, J. Zhu and Y. Wan, *J. Mol. Catal. A: Chem.*, 2005, **226**, 93.

6 (*a*) P. D. Yang, D. Y. Zhao, D. I. Margolese, B. F. Chmelka and G. D. Stucky, *Nature*, 1998, **396**, 152; (*b*) G. Garnweitner, B. Smarsly, R. Assink, W. Ruland, E. Bond and C. J. Brinker, *J. Am. Chem. Soc.*, 2003, **125**, 5626; (*c*) D. A. Doshi, A. Gibaud, V. Goletto, M. Lu, H. Gerung, B. Ocko, S. M. Han and C. J. Brinker, *J. Am. Chem. Soc.*, 2003, **125**, 11646.

7 W. K. Ho, J. C. Yu, J. Lin, J. G. Yu and P. S. Li, *Langmuir*, 2004, **20**, 5865.

8 A. Badalyan and P. Pendleton, *Langmuir*, 2003, **19**, 7919.

9 (*a*) D. R. Rolison, *Science*, 2003, **299**, 1698; (*b*) A. T. Bell, *Science*, 2003, **299**, 1688.

10 X. C. Wang, J. C. Yu, C. M. Ho and A. C. Mak, *Chem. Commun.*, 2005, **17**, 2262.

11 (*a*) I. Justicia, P. Ordejon, G. Canto, J. L. Mozos, J. Fraxedas, G. A. Battiston, R. Gerbasi and A. Figueras, *Adv. Mater.*, 2002, **14**, 1399; (*b*) M. R. Hoffmann, S. T. Martin, W. Choi and D. W. Bahnemann, *Chem. Rev.*, 1995, **95**, 69.

12 (*a*) E. Borgarello, J. Kiwi, M. Gratzel, E. Pelizzetti and M. Visca, *J. Am. Chem. Soc.*, 1982, **104**, 2996; (*b*) N. Serpone, D. Lawless, J. Disdier and J. M. Herrmann, *Langmuir*, 1994, **10**, 643; (*c*) L. Palmisano, V. Augugliaro, A. Sclafani and M. Schiavello, *J. Phys. Chem.*, 1988, **92**, 6710.